Insight into $Y@X_2B_8$ (Y= Li, CO_2 and Li-CO_2, X = Be, B and C) nanostructures:

A computational study

Ipak Torkpoor[a], Musa Heidari Nezhad Zanjanpour[a], Navid Salehi[b], Fatemeh Gharibzadeh[b], Ladan Edjlali [b,*]

[a] Department of Science, Payame Noor University, P. O. Box: 19395-4697 Tehran, Iran
[b] Department of Chemistry, Tabriz Branch, Islamic Azad University, Tabriz, Iran

ARTICLE INFO

ABSTRACT

The doping of the Li atom and CO_2 molecule to the X_2B_8 (X = Be, B and C) backbones have been carried out on the potential energy surface to provide clear vision on the structural and electronic features of the $Y@X_2B_8$ (Y = Li, CO_2 and Li&CO_2, X = Be, B and C) systems. Our results show that the adsorption energies of the Li atom in the Li@X_2B_8 systems (-1.52 eV ~ -3.05 eV) are much bigger than those of the CO_2 molecule in the CO_2@X_2B_8 systems (-0.10 eV ~ -0.89 eV). Moreover, the B_2B_8 and the Be_2B_8 can be selected as prefer backbones for the adsorption of Li atom and the CO_2 molecule, respectively. Finally, bigger adsorption energy of the Li&CO_2@Be_2B_8 system (-1.06 eV) compared with that of the CO_2@Be_2B_8 system (-0.89 eV) presents that the Li atom doping in the Be_2B_8 backbone increases adsorption energy of the CO_2 molecule. Similar result has been not found for the B_2B_8 and the C_2B_8 backbones.

1. Introduction

Boron is one of the very interesting elements in the periodic Table. Pure boron molecules are intermediate compounds between the materials with purely nonmetallic and metallic characteristics. This feature results into high chemical flexibility of boron rich molecules and it motives many researchers to search the ground-state geometries of boron rich molecules and reveal their unique characteristics [1-8].

The organized investigation has been carried out by Boustani [9] on possible structural geometries of the B_n (n = 2−14) molecules. The results show that the B_{10} molecule can have three different configurations of the convex B_{10} (C_{2v}), the quasiplanar B_{10} (C_{2h}) and the nonplanar B_{10} (C_s) on the singlet potential energy surface (PES). Moreover, the quasiplanar B_{10} (C_{2h}) molecule contains two different fragments in its structural geometry and is more stable than two other configurations. The quasiplanar B_{10} (C_{2h}) molecule has the planar ring with eight B-atoms along with two central B atoms which locate up and under planar ring.

Note that the central B atoms of the B_{10} (C_{2h}) molecule have strong chemical bonds with those of planar ring. [9] It is necessary to say that the replacement of two central B atoms of the quasiplanar B_{10} (C_{2h}) molecule with either two more electropositive atoms of the Be, denoted as the nonplanar Be_2B_8 (D_{8h}) molecule, or two more electronegative atoms of the C, denoted as the planar C_2B_8 (D_{2h}) molecule, has been carried out by Frenking et al. [10-11] The C_2B_8 (D_{2h}) molecule has been found to be the planar molecule [10]. This means that the replacement of two central B atoms of the quasiplanar B_{10} (C_{2h}) molecule with those of C atoms causes to incorporation of the central C_2 unit in the sheet of the planar C_2B_8 (D_{2h}) molecule. In the planar C_2B_8 (D_{2h}) molecule, the strong chemical bonds can be observed between the central C_2 unit and the peripheral B atoms [10]. Different from the planar C_2B_8 (D_{2h}) molecule, the replacement of the central B_2 unit of the quasiplanar B_{10} (C_{2h}) molecule with two Be atoms causes to form the nonplanar Be_2B_8 (D_{8h}) molecule [11] which contains the symmetric ring through eight B atoms in which two Be atoms are vertical to the B atoms ring. The stability

factor of the nonplanar Be_2B_8 (D_{8h}) molecule is the strong chemical bonds between Be and B atoms. These B−Be bonds act such as the wheel spokes and cause to unusual short Be−Be distance. In spite of very short Be−Be distance, no bond critical point (BCP) has been observed between the two Be atoms of the nonplanar Be_2B_8 (D_{8h}) molecule [11].

In the present paper, our main objective is to increase adsorption energy of the CO_2 molecule in X_2B_8 (X = Be, B and C) species. In this regard, high electron deficiency of X_2B_8 (X = Be, B and C) molecules motivated us to use the Li atom as good electron donor in the X_2B_8 (X = Be, B and C) species.

Therefore, in first step, we have doped the Li atom to the X_2B_8 (X = Be, B and C) species to report the possible local minima to reveal the electronic and structural features of the $Li@X_2B_8$ (X = Be, B and C) species. In second step, we have revealed geometry and adsorption energy of $CO_2@X_2B_8$ and $Li\&CO_2@X_2B_8$ (X = Be, B and C) species to carry out the comparative study on adsorption energy of the $Y@X_2B_8$ (Y=Li, CO_2 and Li-CO_2, X = Be, B and C) molecules to find the influence of Li-atom in the adsorption energy of CO_2 molecule.

2. Computational details

At first, we have carried out re-optimization for the most stable structures of the Be_2B_8 (D_{8h}), the B_2B_8 (C_{2h}) and the C_2B_8 (D_{2h}) molecules at the RMP2/6-311+G(d) level. Subsequently, the Li and CO_2 have been added to the optimized geometries of the Be_2B_8 (D_{8h}), the B_2B_8 (C_{2h}) and the C_2B_8 (D_{2h}) molecules in the different positions to obtain all possible local minima of the $Y@X_2B_8$ (Y=Li, CO_2 and Li-CO_2, X = Be, B and C) molecules on the singlet or doublet PESs at the R(U)MP2/6-311+G(d) level. In the next step, we have carried out the calculations of single-point energy on the optimized geometries at the R(U)MP2/aug-cc-pVDZ level to provide more reliable energies. Additionally, all vibrational frequencies of the reported local minima have been checked at the R(U)MP2/6-311+G(d) level to confirm the optimized geometries as valid local minima. Subsequently, information on the bond critical points (BCPs) and the difference map of electron density have been obtained through the AIM2000 [12] and the multiwfn [13] softwares, respectively. Finally, we have calculated the values of β_{total} at the ROMP2/aug-cc-pVDZ//UMP2/6-311+G(d) level through the code developed by Kurtz et al. [14]

in which the magnitude of the electric field is 0.0010 a.u. Note that we have used GAMESS [15] in the present paper. This research work is in continuation of our previous works on nanotechnology [16-30].

3. Results and discussions

3.1. The addition of Li atom to X_2B_8 (X = Be, B and C) species

The doping of Li atom, a well-known electron donor to molecules can lead to significant changes in their electronic and structural properties. In the present paper, we have added Li atom to the X_2B_8 (X = Be, B and C) molecules to investigate electronic and structural features of the $Li@X_2B_8$ (X = Be, B and C) molecules on the doublet PES. As shown in Figure 1, we have only found two (the Be_2B_8-Li-α and the Be_2B_8-Li-β molecules), three (the B_2B_8-Li-α, the B_2B_8-Li-β and the Be_2B_8-Li-γ molecules) and one (the C_2B_8-Li molecule) structures due to the doping of the Li atom to the Be_2B_8 (D_{8h}), the B_2B_8 (C_{2h}) and the C_2B_8 (D_{2h}) molecules, respectively.
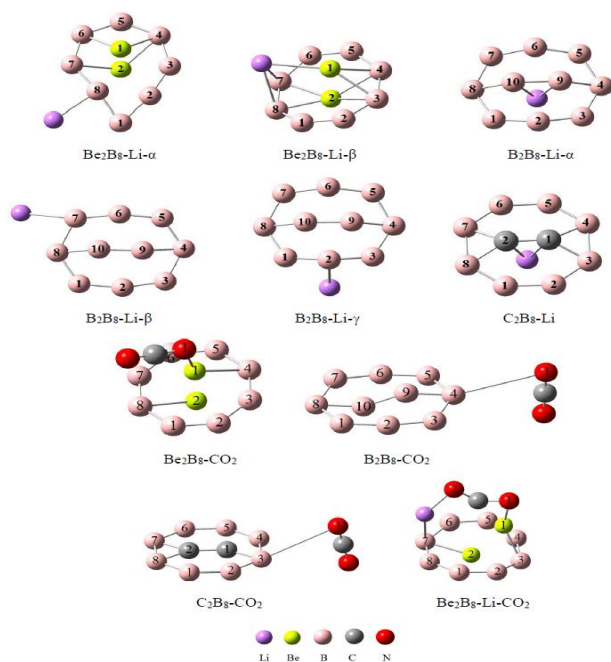

Fig. 1 The obtained structures for the $Y@X_2B_8$ (Y=Li, CO_2 and Li-CO_2, X = Be, B and C) molecules.

3.2. AIM analysis

The atoms in molecules (AIM) theory has been used to search possible BCPs in the $Li@X_2B_8$ (X = Be, B and C) molecules. Based on the AIM analysis, we have displayed atomic connections through solid lines in all molecules in Figure 1. The comparative investigation of the atomic connections in Figure 1 reveals two significant points. Firstly, there is no interaction (through the BCPs) between two Be atoms in the Be_2B_8-Li-α and the Be_2B_8-Li-β molecules. This result is in agreement with lack of the Be-Be interaction in the Be_2B_8 (D_{8h}) molecule reported by Frenking et al. [11] This means that the addition of the Li atom to the Be_2B_8 (D_{8h}) molecule, denoted as the Be_2B_8-Li-α and the Be_2B_8-Li-β molecules, results into no interaction between Be atoms. Secondly, all $Li@X_2B_8$ (X = Be, B and C) molecules include the Li-B interaction except for the C_2B_8-Li molecule. In the C_2B_8-Li molecule, the Li

atom has no interaction with the B atoms as shown in Figure 1. Subsequently, we have listed the values of the electron density (p(r)) and $\nabla^2\rho$(r) in the BCPs of Li-Be, Li-B and Li-C interactions in Table S1 in electronic supporting information (ESI). From Table S1, the ranges 0.0141 a.u ~ 0.0270 a.u and 0.0406 a.u ~ 0.1419 a.u have been found for the p(r) and $\nabla^2\rho$(r), respectively. The small values reported of p(r) and the positive values of $\nabla^2\rho$(r) confirm that the interaction between the Li atom and other atoms (Be, B and C) in the Li@X_2B_8 (X = Be, B and C) molecules are weak and non-covalent. Note that the strongest interaction of the Li atom among all reported interactions of the Li atom in the Li@X_2B_8 (X = Be, B and C) molecules belongs to the Li-B interaction in the Be$_2B_8$-Li-α molecule with the bond length of 2.07 Å which is the shortest bond length (2.07 Å) for the interaction of the Li in the Li@X_2B_8 (X = Be, B and C) molecules.

3.3. Stability

The adsorption and vertical ionization (VI) energies for all local minima of the Li@X_2B_8 (X = Be, B and C) molecules have been presented in Figure 2 and listed in Table S2 of the ESI. According to Figure 2, the range of the adsorption energies for the six local minima is -1.52 eV ~ -3.05 eV due to doping of Li atom. Moreover, the ranking of the reported adsorption energies is B$_2B_8$-Li-α > Be$_2B_8$-Li-γ > B$_2B_8$-Li-β > Be$_2B_8$-Li-β > C$_2B_8$-Li > Be$_2B_8$-Li-α. Note that three bigger adsorption energies among all reported adsorption energies belong to the B$_2B_8$-Li-α, the B$_2B_8$-Li-β and the Be$_2B_8$-Li-γ molecules, the Li@B_2B_8 system. This means that the doping of the Li atom to the B$_2B_8$ (C$_{2h}$) causes the molecules with bigger adsorption energies (higher thermodynamic stability) compared to that of the Be$_2B_8$ (D$_{8h}$) and the C$_2B_8$ (D$_{2h}$) molecules. Additionally, the calculated results show that the values of the VI energy for the Li@X_2B_8 (X = Be, B and C) molecules are in narrow range 6.89 eV ~ 7.19 eV. These big values show that the Li@X_2B_8 (X = Be, B and C) molecules are not appropriate electron donor in the electron transfer reactions. Additionally, the fluctuation of the reported VI energies is very small as shown in Figure 2.

As known, the HOMO and the LUMO energy and their corresponding gaps provide more clear vision on the ability of an electron transfer from the HOMO to the LUMO. In Table S3 of the ESI, we have listed the HOMO and the LUMO energies for both sets α and β of the Li@X_2B_8 (X = Be, B and C) molecules on the doublet PES and set α of the Be$_2B_8$ (D$_{8h}$), the B$_2B_8$ (C$_{2h}$) and the C$_2B_8$ (D$_{2h}$) molecules on the singlet PES and their corresponding energy gaps. According to Figure 3, the doping of Li atom to all the Be$_2B_8$ (D$_{8h}$), the B$_2B_8$ (C$_{2h}$) and the C$_2B_8$ (D$_{2h}$) molecules causes to decrease energy gap of HOMO-LUMO. The biggest and smallest energy gaps due to doping of the Li atom

belong to the B$_2B_8$-Li-α (7.49 eV) and the B$_2B_8$-Li-β (6.08 eV) molecules, respectively. As known, the HOMO-LUMO energy gap reflects the chemical stability of the molecules. This means that the B$_2B_8$-Li-α molecule has the highest chemical stability among all the reported Li@X_2B_8 (X = Be, B and C) molecules. As shown in Figures 4 and 5, the HOMOs locate on the Be$_2B_8$, the B$_2B_8$ and the C$_2B_8$ backbones in the Li@X_2B_8 (X = Be, B and C) molecules. In contrast, the distribution of the LUMOs is mainly on the Li atom except for the C$_2B_8$-Li molecule. In the C$_2B_8$-Li molecule, the LUMO locates mainly on both the Li and the C atoms.
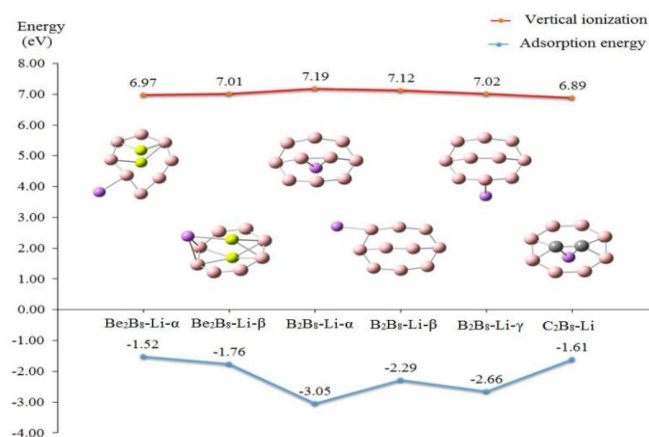

Fig. 2 The adsorption and the vertical ionization energies of all the obtained molecules for the Li@X_2B_8 (X = Be, B and C) molecules.
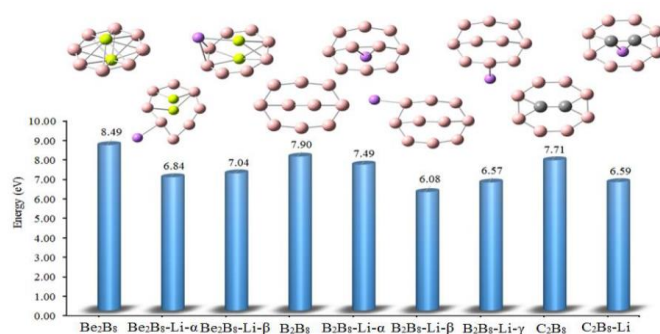

Fig. 3 The HOMO-LUMO energy gap of the obtained structures for the Li@X_2B_8 (X = Be, B and C) molecules along with the Be$_2B_8$ (D$_{8h}$), the B$_2B_8$ (C$_{2h}$) and the C$_2B_8$ (D$_{2h}$) species.
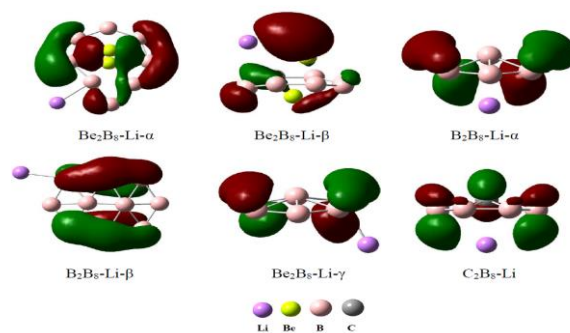

Fig. 4 The distribution of the HOMO in the Li@Be$_2B_8$, the Li@B_2B_8 and the Li@C_2B_8 molecules (isosurface = 0.04).

3.4. NBO charges

The natural bond orbital (NBO) charges as alternative factor can provide clear insight into the atomic electron donor or electron acceptor of the Li@X_2B_8 (X = Be, B and C) molecules.

In this regard, we have listed the NBO charges of all atoms in Table S4 of the ESI. The precise investigation of the NBO charges reveals three significant points. Firstly, the positive range 0.76 e ~ 0.91 e has been found for the NBO charges of the Li atom in the Li@X_2B_8 (X = Be, B and C) molecules. The Li atom of the C_2B_8-Li molecule has the smallest NBO charge (0.76 e) compared to the Li atom of other molecules. Secondly, the Be atoms of the Be_2B_8-Li-α and the Be_2B_8-Li-β molecules and the C atoms of the C_2B_8-Li molecule have positive and negative NBO charges, respectively.

These results show that the Li (and the Be) and the C atoms have the role of electron donor and electron acceptor, respectively in the Li@X_2B_8 (X = Be, B and C) molecules. Thirdly, in the Be_2B_8-Li-α, the Be_2B_8-Li-β and the B_2B_8-Li-α molecules, all B atoms have the negative NBO charges except for the B1 atom of the Be_2B_8-Li-α molecule. In contrast, all the B atoms of the C_2B_8-Li molecule have the positive NBO charges as shown in Table S4 of the ESI. It is very interesting to say that the B atoms of the B_2B_8 backbone in the B_2B_8-Li-β and the Be_2B_8-Li-γ molecules can have both positive and negative NBO charges. On the other words, the B atoms of the Li@X_2B_8 (X = Be, B and C) molecules can play both roles of electron donor and electron acceptor confirming their high chemical flexibility.
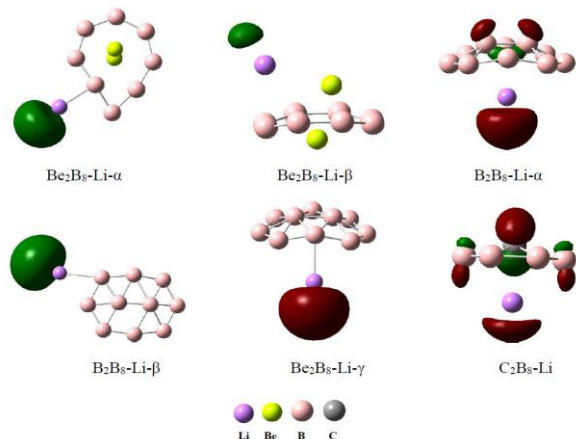

Fig. 5 The distribution of the LUMO in the Li@Be_2B_8, the Li@B_2B_8 and the Li@C_2B_8 molecules (isosurface = 0.04).

3.5. Spin density

All the reported molecules in the Li@X_2B_8 (X = Be, B and C) system are the local minima on the doublet PES containing one odd electron. Therefore, the identification of the odd electron distribution in the Li@X_2B_8 (X = Be, B and C) molecules can help to provide more clear vision about the electronic features of the reported molecules. Figure 6 presents that in the Be_2B_8-Li-α and the Be_2B_8-Li-β molecules, the odd electron locates on either the B or the Be atom. In contrast, the delocalization of the odd electron has been observed on some B atoms of the B_2B_8 backbone in the B_2B_8-Li-α, the B_2B_8-Li-β and the Be_2B_8-Li-γ molecules. In the C_2B_8-Li molecule, the odd electron distributes only on two central C atoms. This means that none of the B atoms in the C_2B_8 backbone collaborate in the distribution of the odd electron.

3.6. Electron transfer (ET)

The addition of the Li atom to the X_2B_8 (X = Be, B and C) molecules changes electron density in both Li atom and the X_2B_8 (X = Be, B and C) molecules. The source of these electron density changes is the electron transfer (ET). In the present paper, we have given a picture of the difference map of electron density between the Li@X_2B_8 (X = Be, B and C) molecules and two fragments of the Li atom and the X_2B_8 (X = Be, B and C) molecules in Figure 7 to provide the appropriate vision on the regions with the increasing or decreasing electron density due to the Li atom doping. It is necessary to say that the regions with the increasing (decreasing) electron density in Figure 7 have been presented through the green (red) regions. Figure 7 shows that electron density of the Li atom decreases in all Li@X_2B_8 (X = Be, B and C) molecules. This means that the Li atom plays the role of the electron donor in all reported molecules. In the Be_2B_8-Li-α and the Be_2B_8-Li-β molecules, the electron density changes of the Be_2B_8 backbone due to doping of the Li atom have been observed mainly in the Be and the B atoms close to the Li atom which reflects these atoms are the main responsible for the ET. Additionally, the difference map of electron density in the B_2B_8-Li-α, the B_2B_8-Li-β and the Be_2B_8-Li-γ molecules is much more different than that of the Be_2B_8-Li-α and the Be_2B_8-Li-β molecules as shown in Figure 7. In three molecules of the B_2B_8-Li-α, the B_2B_8-Li-β and the Be_2B_8-Li-γ, all B atoms of the B_2B_8 backbone include the changes of electron density due to the Li atom doping. On the other words, all atoms of the Li@B_2B_8 molecules have the significant collaboration in the ET. Different from the Be_2B_8-Li-α, the Be_2B_8-Li-β, the B_2B_8-Li-α, the B_2B_8-Li-β and the Be_2B_8-Li-γ molecules, the changes of the electron density have been observed mainly in two central C atoms of the C_2B_8-Li molecule as shown in Figure 7. Indeed, the B atoms of the C_2B_8 backbone have the minor role in the ET.

3.7. The first hyperpolarizability

Nowadays, the materials with the nonlinear optical (NLO) properties obtain the great attentions by researchers [31-38].

The first hyperpolarizability (β_{total}) is the significant criterion to identify materials with the NLO properties.
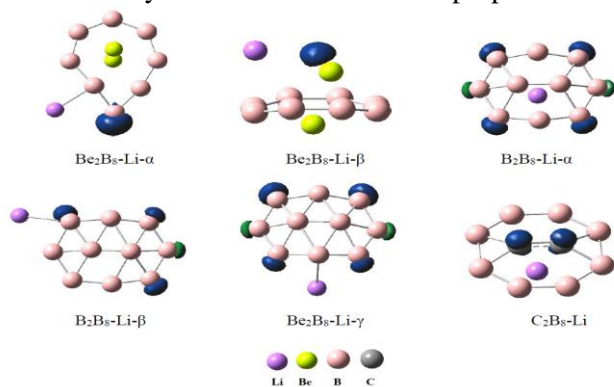

Fig. 6 The distribution of spin density in the Li@Be$_2$B$_8$, the Li@B$_2$B$_8$ and the Li@C$_2$B$_8$ molecules (isosurface = 0.02).

To achieve this purpose, we have listed the values of β_{total} and their components in Table S5 of the ESI and displayed in Figure 8. The calculated results show that β_{total} values of the Li@X$_2$B$_8$ (X = Be, B and C) molecules are in the range 50 a.u ~ 2200 a.u at the ROMP2 level. The smallest and the biggest β_{total} values have been observed for the B$_2$B$_8$-Li-α (50 a.u) and the B$_2$B$_8$-Li-β (2200 a.u) molecules. Additionally, the obtained β_{total} values for B$_2$B$_8$-Li-α (50 a.u), B$_2$B$_8$-Li-β (2200 a.u) and Be$_2$B$_8$-Li-γ (457 a.u) molecules reflect severe dependence between the β_{total} value and the Li atom position on the B$_2$B$_8$ backbone. Finally, the β_{total} value of the Li@Be$_2$B$_8$ molecules, 1085 a.u and 1257 a.u, are bigger than that of the Li@C$_2$B$_8$ molecule, 1079 a.u.
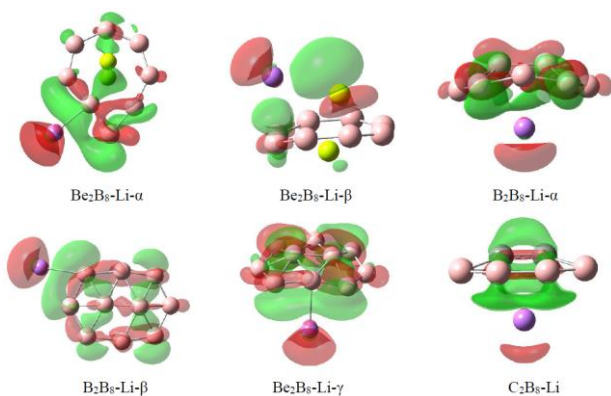

Fig. 7 The difference map of electron density in the Li@X$_2$B$_8$ (X = Be, B and C) molecules (The green (+0.003 a.u.) and red (-0.003 a.u.) regions show the increasing and decreasing electron density, respectively).

Our results in the previous part show that the adsorption energy in the Li@X$_2$B$_8$ (X = Be, B and C) species is bigger than that of CO$_2$@X$_2$B$_8$ (X = Be, B and C) species. This means that we can obtain the most stable geometries of the Li&CO$_2$@X$_2$B$_8$ (X = Be, B and C) species through addition of the CO$_2$ molecule to the Li@X$_2$B$_8$ (X = Be, B and C) species.
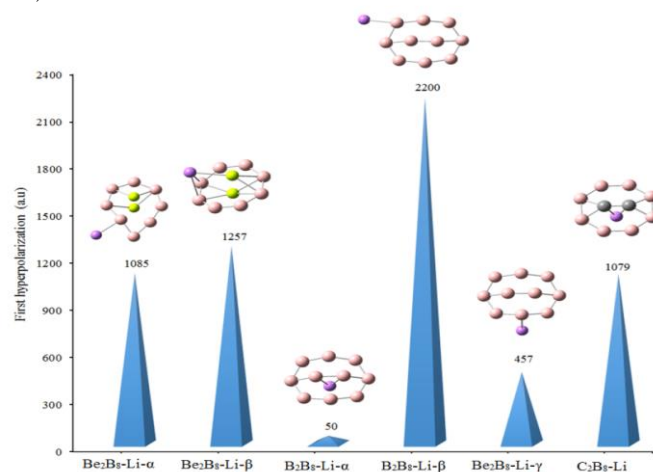

Fig. 8 The values of the first hyperpolarizability for the Li@X$_2$B$_8$ (X = Be, B and C) molecules.

3.8. The addition of both Li atom and CO$_2$ molecule to X$_2$B$_8$ (X = Be, B and C) species

In this regard, we have added the CO$_2$ molecule to different positions of Be$_2$B$_8$-Li-β, B$_2$B$_8$-Li-α and C$_2$B$_8$-Li spices. In spite of numerous attempts, we have found no suitable local minima for CO$_2$@B$_2$B$_8$-Li-α and CO$_2$@C$_2$B$_8$-Li spices. Indeed, all optimized geometries for the CO$_2$@B$_2$B$_8$-Li-α and the CO$_2$@C$_2$B$_8$-Li spices in the present paper include either imaginary frequency or positive adsorption energy. In contrast, one local minimum has been found through the addition of the CO$_2$ molecule to the Be$_2$B$_8$-Li-β species, shown as the Be$_2$B$_8$-Li-CO$_2$ species in Figure 1. The interaction of the Li and Be atoms with O atoms of the bent CO$_2$ molecule can be considered in the Be$_2$B$_8$-Li-CO$_2$ species. Our results show that the adsorption energy of the CO$_2$ molecule on the Be$_2$B$_8$-Li-β in the Be$_2$B$_8$-Li-CO$_2$ species is -1.06 eV. The comparison of the adsorption energy of the CO$_2$ molecule in the Be$_2$B$_8$-Li-CO$_2$ species (-1.06 eV) with that of the Be$_2$B$_8$-CO$_2$ species (-0.89 eV) confirms that the doping of the Li atom in the Be$_2$B$_8$ causes to increase adsorption energy of the CO$_2$ molecule. Similar result has been not found for the B$_2$B$_8$ and the C$_2$B$_8$ species.

4. Conclusions

In the present paper, we have carried the addition of the Li atom and CO$_2$ molecule to the nonplanar Be$_2$B$_8$ (D$_{8h}$), the quasiplanar B$_2$B$_8$ (C$_{2h}$) and the planar C$_2$B$_8$ (D$_{2h}$) molecules on the singlet or doublet PESs. The obtained results can be listed as follows:

a) Two, three, and one structures have been found for the doping of Li atom to the Be$_2$B$_8$ (D$_{8h}$), the B$_2$B$_8$ (C$_{2h}$) and the C$_2$B$_8$ (D$_{2h}$) molecules, respectively. The AIM analysis of the Li@X$_2$B$_8$ (X = Be, B and C) molecules shows that the interactions between the Li atom and the backbones of the Be$_2$B$_8$, the B$_2$B$_8$ and the C$_2$B$_8$ are weak and non-covalent. Additionally, no bond path has been

found between two the Be atoms of the Li@Be$_2$B$_8$ molecules.

b) According to the adsorption energies of the Li atom, -1.52 eV ~ -3.05 eV, the thermodynamic stability of the Li@B$_2$B$_8$ molecules are much bigger than that of the Li@Be$_2$B$_8$ and the Li@C$_2$B$_8$ molecules. Therefore, the B$_2$B$_8$ species is more suitable for doping of the Li atom.

c) No significant difference exists among the VI energies of the Li@X$_2$B$_8$ (X = Be, B and C) molecules. Additionally, big values of VI show that the Li@X$_2$B$_8$ (X = Be, B and C) molecules are not appropriate electron donor in the electron transfer reactions.

d) The energy gap of the HOMO-LUMO in all the Be$_2$B$_8$ (D$_{8h}$), the B$_2$B$_8$ (C$_{2h}$) and the C$_2$B$_8$ (D$_{2h}$) molecules decreases due to doping of Li atom. The biggest energy gap among the reported Li@X$_2$B$_8$ (X = Be, B and C) molecules belongs to the B$_2$B$_8$-Li-α molecule of the Li@B$_2$B$_8$ system.

e) The positive NBO charges of the Li and the Be atoms and that of negative in the C atoms reflect the roles of electron donor and electron acceptor for the Li (and the Be) and the C atoms in the Li@X$_2$B$_8$ (X = Be, B and C) molecules, respectively. In contrast, the B atoms have dual role. Indeed, they can accept both roles of electron donor and electron acceptor in the Li@X$_2$B$_8$ (X = Be, B and C) molecules which confirms high chemical flexibility of the B atoms.

f) The investigation of the spin density distribution reveals that the odd electron of the Li@B$_2$B$_8$ molecules is much less locale than that of the Li@Be$_2$B$_8$ and the Li@C$_2$B$_8$ molecules.

g) Although, the different atoms involve in the electron transfer, the overall tendency of the electron transfer is from the Li atom to the Be$_2$B$_8$, the B$_2$B$_8$ and the C$_2$B$_8$ backbones in all Li@X$_2$B$_8$ (X = Be, B and C) molecules.

h) The β$_{total}$ values of the Li@X$_2$B$_8$ (X = Be, B and C) molecules are in the range 50 a.u ~ 2200 a.u. Moreover, the calculated results reveals that the β$_{total}$ value of the Li@B$_2$B$_8$ molecules has severe dependence to the Li atom position on the B$_2$B$_8$ backbone.

i) That the adsorption energy of the CO$_2$ molecule on the Be$_2$B$_8$ species (-0.89 eV) is much bigger than that of the B$_2$B$_8$ (-0.10 eV) and C$_2$B$_8$ (-0.11 eV) species. Therefore, the Be$_2$B$_8$ species is more prefer than the B$_2$B$_8$ and the C$_2$B$_8$ species in order to adsorb the CO$_2$ molecule.

k) The results show that the values of the adsorption energy of the Li atom (-1.52 eV ~ -3.05 eV) are much bigger than those of the CO$_2$ molecule (-0.10 eV ~ -0.89 eV). Therefore, the adsorption of the Li atom in the X$_2$B$_8$ (X = Be, B and C) species is more prefer than that of the CO$_2$ molecule.

m) The doping of the Li atom in the Be$_2$B$_8$ species causes to increase adsorption energy of the CO$_2$ molecule. Similar result has been not found for B$_2$B$_8$ and

C$_2$B$_8$ species. Therefore, the Be$_2$B$_8$ species is more prefer than the B$_2$B$_8$ and the C$_2$B$_8$ species in order to adsorb both Li atom and CO$_2$ molecule.

References

[1] H. Tang, S. Ismail-Beigi; Novel precursors for boron nanotubes: The competition of two-center and three-center bonding in boron sheets; *Phys. Rev. Lett.* 99 (2007) 115501–115504.

[2] H.J. Zhai, A.N. Alexandrova, K.A. Birch, A.I. Boldyrev, L.S. Wang, hepta-and octacoordinate boron in molecular wheels of eight-and nine-atom boron clusters: observation and confirmation; *Angew. Chem. Int. Ed.*; 42 (2003) 6004–6008.

[3] Z.A. Piazza, H.S. Hu, W.L. Li, Y.F. Zhao, J. Li, L.S. Wang; Planar hexagonal B$_{36}$ as a potential basis for extended single-atom layer boron sheets; *Nat. Commun.* 5 (2014) 3113–3119.

[4] A. Muñoz-Castro, I.A. Popov, A.I. Boldyrev, Long-range magnetic response of toroidal boron structures: B$_{16}$ and [Co@B$_{16}$]$^{-/3-}$ species; *Phys. Chem. Chem. Phys.* 19 (2017) 26145-26150.

[5] J. Kunstmann, A. Quandt, Broad boron sheets and boron nanotubes: An ab initio study of structural, electronic, and mechanical properties; *J. Phys. Rev. B*; 74 (2006) 035413–035427.

[6] K.C. Lau, R. Pandey, Thermodynamic stability of novel boron sheet configurations, *J. Phys. Chem. B*; 112 (2008) 10217–10220.

[7] W. An, S. Bulusu, Yi. Gao, X.C. Zeng, Relative stability of planar versus double-ring tubular isomers of neutral and anionic boron cluster B$_{20}$ and B$_{20}^-$; *J. Chem. Phys.* 124 (2006) 154310-154316.

[8] X-M. Luo, T. Jian, L-J. Cheng, W-L. Li, Q. Chen, R. Li, H-J. Zhai, S-D. Li, A.I. Boldyrev, J. Li, L-S. Wang, B$_{26}^-$: The smallest planar boron cluster with a hexagonal vacancy and a complicated potential landscape, *Chem. Phys. Lett.* 683 (2017) 336-341.

[9] I. Boustani, Systematic ab initio investigation of bare boron clusters:mDetermination of the geometry and electronic structures of (n=2–14), *Phys. Rev.* B; 55 (1997) 16426-16438.

[10] S. Erhardt, G. Frenking, Z. Chen, P.R. Schleyer, Aromatic boron wheels with more than one carbon atom in the center: C$_2$B$_8$, C$_3$B$_9^{3+}$, and C$_5$B$_{11}^+$; *Angew. Chem. Int. Ed.* 44 (2005) 1078–1082.

[11] Z.h. Cui, W.S. Yang, L. Zhao, Y. Ding, G. Frenking, Unusually Short Be− Be Distances with and without a Bond in Be$_2$F$_2$ and in the Molecular Discuses Be$_2$B$_8$ and Be$_2$B$_7^-$; *Angew. Chem.* 128 (2016) 7972–7977.

[12] F. Biegler-König, J. Schönbohm, AIM2000 Program Package Ver. 2.0. University of Applied Sciences Bielefeld, (2002).

[13] T. Lu, F. Chen, Multiwfn: a multifunctional wave function analyzer, *J. Comput. Chem.* 33 (2015) 580–592.

[14] H.A. Kurtz, J.J.P. Stewart, K.M. Dieter; Calculation of the nonlinear optical properties of molecules; *J. Comput. Chem.* 11 (1990) 82–87.

[15] M.W. Schmidt, K.K. Baldridge, J.A. Boatz, S.T. Elbert, M.S. Gordon, J.H. Jensen, S. Koseki, N. Matsunaga, K.A.

Nguyen, S.J. Su, T.L. Windus, M. Dupuis, Montgomery JA; General atomic and molecular electronic structure system, *J. Comput. Chem.* 14 (1993) 1347–1363.

[16] E. Vessally, S. Soleimani–Amiri, A. Hosseinian, L. Edjlali and A. Bekhradnia A comparative computational study on the BN ring doped nanographenes, *Appl. Surf. Sci.*, 396 (2017) 740–745;

[17] K. Nejati, A. Hosseinian, L. Edjlali and E. Vessally, The effect of structural curvature on the cell voltage of BN nanotube based Na–ion batteries, *J. Mol. Liq.*, 229 (2017) 167–171;

[18] L. Safari, E. Vessally, A. Bekhradnia, A. Hosseinian and L. Edjlali, A DFT study on the sensitivity of two–dimensional BN nanosheet to nerve agents cyclosarin and tabun, *Thin Solid Films*, 623 (2017) 157–163;

[19] S. A. Siadati, E. Vessally, A. Hosseinian and L. Edjlali, Possibility of sensing, adsorbing, and destructing the Tabun–2D–skeletal (Tabun nerve agent) by C_{20} fullerene and its boron and nitrogen doped derivatives, *Synthetic Met.*, 220 (2016) 606–611;

[20] E. Vessally, F. Behmagham, B. Massoumi, A. Hosseinian and L. Edjlal, Carbon nanocone as an electronic sensor for HCl gas: Quantum chemical analysis, *Vacuum*, 134 (2016) 40–47;

[21] S. Bashiri, E. Vessally, A. Bekhradnia, A. Hosseinian and L. Edjlali, Utility of extrinsic [60] fullerenes as work function type sensors for amphetamine drug detection: DFT studies, *Vacuum*, 136 (2017) 156–162;

[22] F. Behmagham, E. Vessally, B. Massoumi, A. Hosseinian and L. Edjlali A computational study on the SO_2 adsorption by the pristine, Al, and Si doped BN nanosheets, *Superlattices Microstruct.*, 100 (2016) 350–357;

[23] E. Vessally, S. A. Siadati, A. Hosseinian and L. Edjlali, Selective sensing of ozone and the chemically active gaseous species of the troposphere by using the C_{20} fullerene and graphene segment, *Talanta*, 162 (2017) 505–510;

[24] E. Vessally, S. Soleimani–Amiri, A. Hosseinian, L. Edjlali and A. Bekhradnia The Hartree–Fock exchange effect on the CO adsorption by the boron nitride nanocage, *Phys. E*, 87 (2017) 308–311;

[25] A. Hosseinian, A. Bekhradnia, E. Vessally, L. Edjlali, M.D. Esrafili, A DFT study on the central–ring doped HBC nanographenes, *J. Mol. Graph. Model.*, 73 (2017) 101–107;

[26] A. Hosseinian, Z. Asadi, L. Edjlali, A. Bekhradnia, E. Vessally, NO_2 sensing properties of a borazine doped nanographene: A DFT study, *Comput. Theor. Chem.*, 1106 (2017) 36–42;

[27] K. Nejati, A. Hosseinian, A. Bekhradnia, E. Vessally, L. Edjlali, Na–ion batteries based on the inorganic BN nanocluster anodes: DFT studies, *J. Mol. Graph. Model.*, 74 (2017) 1–7;

[28] K. Nejati, A. Hosseinian, E. Vessally, A. Bekhradnia, L. Edjlali, A comparative DFT study on the interaction of cathinone drug with BN nanotubes, nanocages, and nanosheets, *Appl. Surf. Sci.*, 422 (2017) 763–768;

[29] K. Nejati, A. Hosseinian, E. Vessally, A. Bekhradnia, L. Edjlali, A theoretical study on the electronic sensitivity of the pristine and Al-doped $B_{24}N_{24}$ nanoclusters to F_2CO and Cl_2CO gases, *Struct. Chem.*, 28 (2017) 1919–1926;

[30] N. Salehi, L. Edjlali, E. Vessally, I. Alkorta, M. Es'haghi, Lin@Tetracyanoethylene (n=1–4) systems: Lithium salt vs lithium electride, *Comput. Theor. Chem.*, 1149 (2019)17–23.

[31] P. Karamanis, C. Pouchan, fullerene–C60 in contact with alkali metal clusters: prototype nano-objects of enhanced first hyperpolarizabilities; *J. Phys. Chem. C* 116 (2012) 11808–11819.

[32] C. Tu, G. Yu, G. Yang, X. Zhao, W. Chen, S. Li, X. Huang, Constructing (super) alkali–boron-heterofullerene dyads: an effective approach to achieve large first hyper polarizabilities and high stabilities in $M_3O–BC_{59}$ (M = Li, Na and K) and K@n-BC_{59} (n = 5 and 6); *Phys. Chem. Chem. Phys.* 16 (2014) 1597–1606.

[33] K. Okuno, Y. Shigeta, R. Kishi, M. Nakano, Photochromic switching of diradical character: design of efficient nonlinear optical switches; *J. Phys. Chem. Lett.*, 4 (2013) 2418–2422.

[35] K. Hatua, P.K. Nandi, Beryllium-cyclobutadiene multidecker inverse sandwiches: electronic structure and second-hyperpolarizability, *J. Phys. Chem. A* 117 (2013) 12581–12589.

[36] H.Q. Wu, R.L. Zhong, S.L. Sun, H.L. Xu, Z.M. Su, Alkali metals-substituted adamantanes lead to visible light absorption: large first hyperpolarizability; *J. Phys. Chem. C*; 118 (2014) 6952–6958.

[37] K.B. Eisenthal, Second harmonic spectroscopy of aqueous nano-and microparticle interfaces; *Chem. Rev.* 106 (2006) 1462–1477.

[38] Y.Y. Hu, S.L. Sun, S. Muhammad, H.L. Xu, Z.M. Su, How the number and location of lithium atoms affect the first hyperpolarizability of graphene; *J, Phys, Chem, C* 114 (2010) 19792–19798.

How to Cite This Article